HIGH-SPEED TURBULENT MIXING AND COMBUSTION : MILES VS PHYSICAL LES

Mehmet Karaca
ICARE-CNRS
1c, ave. de la Recherche Scientifique
F-45071 Orléans cedex 2, France
mehmet.karaca@cnrs-orleans.fr

Ivan Fedioun
ICARE-CNRS
1c, ave. de la Recherche Scientifique
F-45071 Orléans cedex 2, France
fedioun@cnrs-orleans.fr

Nicolas Lardjane
CEA, DAM, IDF
F-91297 Arpajon, France
nicolas.lardjane@cea.fr

ABSTRACT

This work reports a numerical experiment designed to address the 4th and 9th questions posed by S.B. Pope (New Journal of Physics, 2004) concerning the respective merits of physical and numerical (or implicit) Large Eddy Simulation (LES and MILES), in the simulation of high speed non-reacting and reacting air/H_2 jets typical of scramjet engines. Numerical simulations are performed at resolutions ranging from $32 \times 32 \times 128$ to $256 \times 256 \times 1024$, using a 5^{th} order WENO scheme. Physical LES are carried out with the Smagorinsky and the Selective Structure Function subgrid models associated to molecular diffusion. Implicit LES are performed with and without molecular diffusion. In the non-reacting case, the Smagorinsky model is too dissipative, even with a low value of the constant, $C_s = 0.1$. The Selective Structure Function leads to better results, but does not show any superiority compared to MILES, whatever the grid resolution. In the reacting case, a molecular viscous cut-off in the simulation is mandatory to set a physical width for the reaction zone in MILES-Euler, hence to achieve grid-convergence.

INTRODUCTION

One major concern with the LES of flows in complex physics or complex geometries is about the intricate interactions between numerics and physical subgrid modeling. A typical example is the numerical simulation of scramjet combustion chambers for airbreathing hypersonic propulsion. Shock waves inherently present in the flow require dissipative numerical schemes for stable simulations. In the LES of such challenging flows, some subgrid scale (SGS) terms are systematically neglected or crudely modeled, and the physically sound part of the SGS model that mimics the small-scale mixing and scalar dissipation rate interacts with the numerical diffusion: both smooth the flow field. Going to the limit, the explicit subgrid model can be turned off in the simulation, keeping only the aforementioned desirable numerical diffusion. This approach -highly controversial in the combustion community- is called implicit LES (ILES), or Monotone Integrated LES (MILES), or *numerical* LES (Grinstein *et al.* (2007)). In this paper, we evaluate different LES and MILES strategies for the simulation of high-speed air/H_2 jets, non-reacting (Eggers (1971)) and reacting (ONERA, LAERTE chamber, Magre & Sabel'nikov (2002); George *et al.* (2006)). Numerical simulations are performed at different resolutions up to $256 \times 256 \times 1024$, using a 5^{th} order WENO scheme[1] for the hyperbolic/Euler part of equations and fourth order central finite difference for viscous terms, with and without explicit sugbrid model. The filtered momentum equation is closed using either the compressible Smagorinsky (Erlebacher *et al.* (1992)) or the Selective Structure Function (SSF, David (1993)) subgrid model. The latter includes a three-dimensionality sensor in order to switch-off the model in the initial laminar development of the jet. SGS terms in the energy and species equations are modeled using unity turbulent Prandtl and Schmidt numbers. Modeling of the subgrid reaction rates is left to the numerical scheme. Thermodynamics is taken from Burcat & Ruscic (2006). The transport model is based on Wilke's formula for the viscosity and thermal conductivity of the mixture, and on the Hirschfelder-Curtiss approximation for the multicomponent diffusion. Partial viscosities, thermal conductivities and binary diffusion coefficients are obtained from the CHEMKIN III model. The air/H_2 chemistry is the 7-species, 7-reversible reactions, chemical scheme of ONERA (Davidenko *et al.* (2006)). The terminology used to designate the different approaches hereafter is :

LES_SM	:	LES with the Smagorinsky model
LES_SSF	:	LES with the SSF model
MILES_NS	:	MILES for the Navier-Stokes equations
MILES_EULER	:	MILES for the Euler equations

[1] Although WENO schemes are not monotone, we will use MILES to designate numerical LES in the sequel of the paper.

NON-REACTING CASE

Physical parameters of the Eggers jet are gathered in table 1. The H_2 injector has internal/external diameters of 11.6/12.7 mm. The computational domain is $Ly \times Lz \times Lx = 70 \times 70 \times 700$ mm^3, x being the axial direction of the jet.

Table 1. Physical parameters for the non-reacting air/H_2 jet. In bold, data from Eggers (1971). Other values are computed.

	H_2 jet	air co-flow
U (m/s)	**1074**	**394**
T_{stat}/T_{tot} (K)	260/**300**	222/**300**
P_{stat}/P_{tot} (kPa)	100/167	100/285
Mach	**0.886**	**1.32**
Re_u (1/m)	$11.6\ 10^6$	$36.6\ 10^6$
Re_{jet}	$1.34\ 10^5$	
M_c	0.44	

Grid resolutions are $Ny \times Nz \times Nx = 32 \times 32 \times 128$, 64×64×256, 128×128×512 and 256×256×512. In the latter case, the computational domain has been shorten to half length, i.e. Lx=350mm. The grid is refined both in the transverse direction toward the jet centerline and in the axial direction toward the inlet. In LES_SM, the Smagorinsky model involves the product $C_s^2\Delta^2 = \lambda^2 h^2$, where Δ is the filter width or turbulence resolution length scale, and $h = (\Delta_x\Delta_y\Delta_z)^{1/3}$ is the grid resolution. Simulations are performed for $\lambda^2 = 0.01$ and $\lambda^2 = 0.02$. Taking the Smagorinsky constant $C_s = 0.1$, this may be interpreted as varying the numerical accuracy from $\Delta/h = 1$ to $\Delta/h = \sqrt{2}$.

A central question is whether or not the explicit subgrid model is still active at the finest grid resolution. An appropriate indicator is the eddy-viscosity ratio μ^t_{sgs}/μ. In a free shear flow, one can consider that the model is active if $\mu^t_{sgs}/\mu \gtrsim 10$. In the boundary layer of a wall-bounded flow, one should rather consider $\mu^t_{sgs}/\mu \gtrsim 1$. Figure 1 shows the instantaneous distribution of μ^t_{sgs}/μ for LES_SM (top) and LES_SSF (bottom). At resolutions 64×64×256 and 128×128×512, models are active in both LES_SM and LES_SSF. The effect of the laminarity sensor in the SSF model is apparent, and the model is globally less dissipative than the Smagorinsky model, although instantaneous and local peak values may be a little higher. At the highest resolution 256×256×512 (half computational domain), the SM model is still active whereas the SSF model has almost vanished. This means that the numerical dissipation of the WENO scheme is responsible for most of the subgrid modeling on the finer grid.

Figure 2 displays, in the left column of sub-figures, the center-line, time-averaged, x-velocity distribution (axial decay) for the different simulations. Right sub-figures show the instantaneous structure of the flow using the Q-criterion, for resolution 128×128×512. Vertical and horizontal contour maps show the pressure field and H_2 mass fractions in the

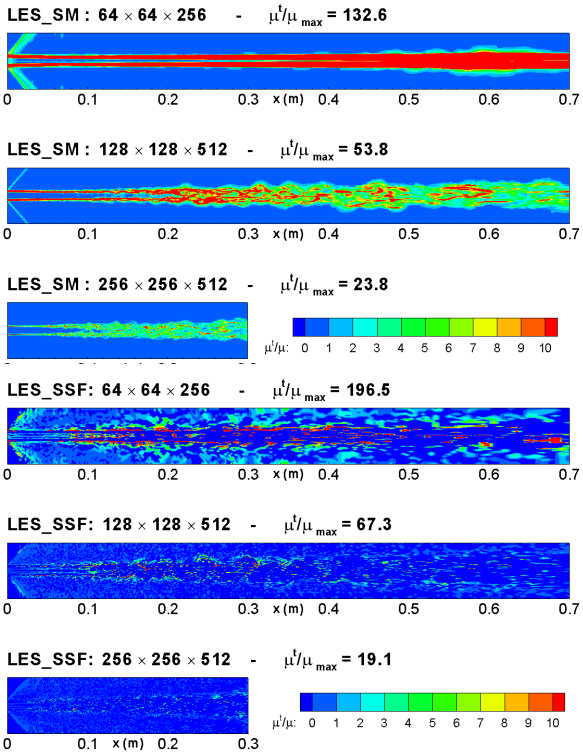

Figure 1. Eddy-viscosity ratio in LES_SM and LES_SSF.

corresponding symmetry planes. For a better visualization, y and z scales are magnified by a factor two. Obviously, the lowest resolution 32×32×128 is inadequate in all the simulations. Increasing the resolution to 64×64×256 improves slightly the results, but the mesh is still too coarse to capture the initial development of shear instabilities. They are damped by the numerical dissipation, and transition is delayed too far downstream. Increasing again the grid resolution up to 128×128×512 improves dramatically the results. All simulations show convergence toward experimental data, except LES_SM with $\lambda^2 = 0.02$ which is still too dissipative. Since the turbulent jet is governed by non-linear inviscid dynamics, MILES_EULER and MILES_NS are very close to each other, but MILES_NS is a little closer to the experiment at the end of the computational domain. At the highest resolution 256×256×512, grid convergence is almost achieved, even with MILES_EULER although there is no physical cutoff in the calculation. The curves are a little wavy because time statistics are not perfectly converged.

The main conclusion for this non-reacting test-case is that conventional LES do not show any superiority compared to MILES, whatever the grid resolution. MILES_EULER and MILES_NS give almost similar results. This means that the computational effort involved in accurate transport models is just wasted when shock capturing schemes are used to solve the compressible Navier-Stokes equations for free shear flows. We were however surprised with MILES_EULER that seems to show grid convergence toward the experimental data although no physical cutoff is present in the simulation. More resolved simulations would be necessary to investigate its asymptotic behavior.

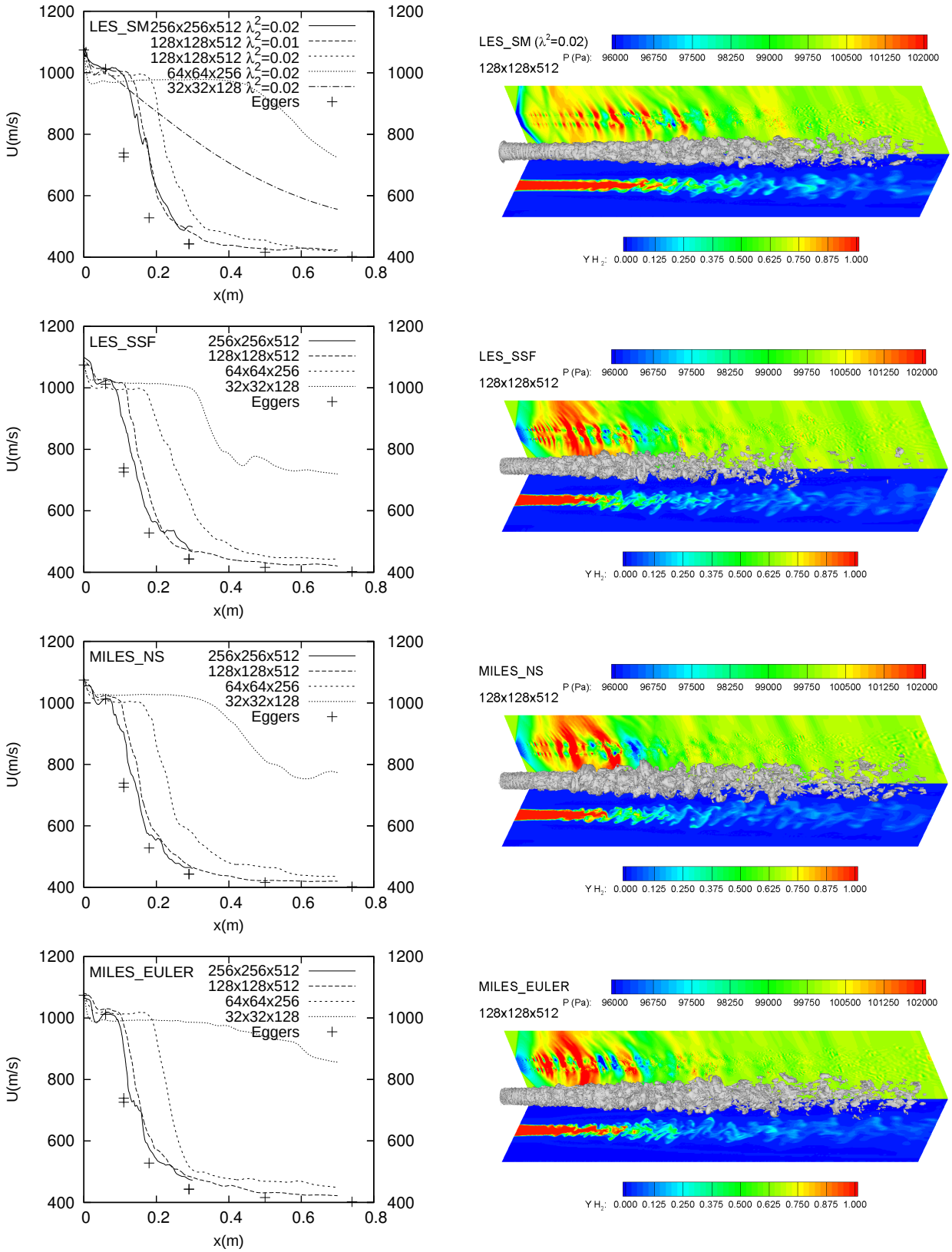

Figure 2. Non-reacting Eggers jet. Left: axial velocity decay, right: instantaneous Q-criterion, pressure and H_2 mass fraction fields. From top to left: LES_SM, LES_SSF, MILES_NS and MILES_EULER.

REACTING CASE

The Mach 2 experimental combustion chamber LAERTE of ONERA, France is designed for the fundamental study of supersonic combustion for air breathing hypersonic propulsion. Experimental studies focus on co-flow vitiation effects on self-ignition delay of the jet. The chemical composition of the vitiated air co-flow is : Y_{O_2}=0.2447, Y_{H_2O}=0.1124, Y_{OH}=2.285×10^{-4}, Y_O=1.8×10^{-5}, $Y_{N_2} = 1-\sum_{others} \approx 0.64265$. Operating conditions are summarized in table 2.

Table 2. LAERTE experimental conditions.

	H_2 jet	air co-flow
U (m/s)	1970	1336
T_{stat}/T_{tot} (K)	160/300	1200/1850
P_{stat}/P_{tot} (kPa)	80/680	80/720
Mach	2	2
$\dot{q}$ (g/s)	6.2	650
Re_{jet}	$2.05\ 10^5$	
M_c	0.39	

The LAERTE chamber has a 45×45 mm^2 constant section of length 370 mm, and then a divergent part with a half-angle of 1.15°. In the present study, only the first part with constant section is simulated. The computational domain is $45\times45\times350$ mm^3. In the simulation, slip-wall boundary conditions are applied to the chamber walls in order to avoid the calculation of turbulent boundary layers. This has an impact on the flow field, but not on the aim of the present study which is to compare LES and MILES results. The H_2 nozzle exit section has a diameter of 6 mm. The inlet velocity profile matches the nozzle solution computed by Davidenko *et al.* (2006) using the RANS approach. One crossing of the computational domain at the co-flow velocity takes approximately 0.27 ms. Simulations have been performed for grid resolutions $64\times64\times256$, $128\times128\times512$ and $256\times256\times1024$. Simulations at the two lowest resolutions have been running for 0.4 ms to clear the flow field before time-averaging of the flow variables for 0.1 ms. Simulation with the $256\times256\times1024$ grid has been running for 0.35 ms before averaging for 0.025 ms only. Because of the poor performance of the Smagorinsky model in the non-reacting case, only LES_SSF, MILES_NS and MILES_EULER have been considered.

Figure 3 displays the subgrid eddy-viscosity ratio in LES_SSF. As in the non-reacting case, the SSF model is still active for the intermediate grid, but has almost no influence on the finest grid. Although the jet Reynolds number is higher, and the convective Mach number is lower than in the Eggers jet, the overall level of subgrid eddy-viscosity is lower in this reacting case than in the non-reacting one. The heat release and subsequent dilatation in the reaction zone inhibits the development of small-scale turbulent structures.

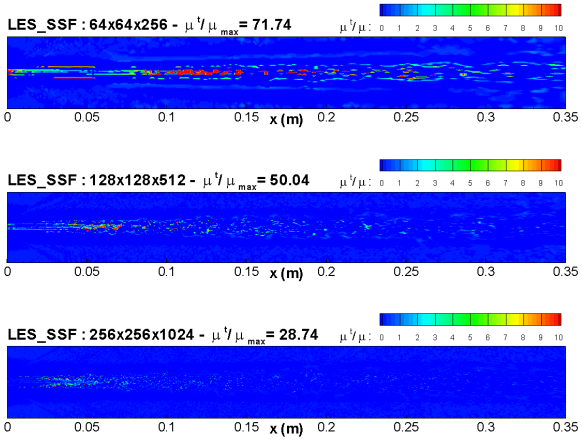

Figure 3. Eddy-viscosity ratio in LES_SSF.

The flame structure is analyzed from the fuel/oxidizer mixture fraction

$$z = \frac{Z - Z^{\text{co-flow}}}{Z^{\text{jet}} - Z^{\text{co-flow}}} \tag{1}$$

where $Z = sY_{H_2} - Y_{O_2}$ is the first of the three Schwab-Zeldovitch variables for a single-step reaction, and $s = Y_{O_2}/Y_{H_2}|_{st} = 8$ is the mass stoichiometric ratio for the H_2/O_2 chemistry. The right column of figure 4 displays, for MILES_NS, the 3-D instantaneous iso-surface of the stoichiometric mixture fraction illustrating the flame location. $z_{st} = 1/(1+\phi_0) = 0.0297$ where $\phi_0 = 32.69$ is the flame equivalence ratio. Vertical and horizontal contour maps are the projections of the instantaneous temperature field and water mass fractions in the corresponding symmetry planes, respectively. Time-averaged radial profiles of temperature at $x = 210$ mm are shown in the left column of figure 4, with experimental measurements from CARS (Coherent Anti-Stokes Raman Scattering). The mean experimental temperature in the center is overestimated, compared to the calculations, because the jet is flapping and the points of measurement are alternatively in the central jet and in the surrounding reaction zone.

The flame region consists of a diffusion layer surrounding the reactive layer, embedding the stoichiometric surface. The reactive layer at the jet/co-flow interface is wrinkled by large-scale turbulent eddies, which bring reactants in contact and mix them at the turbulent level. During that time, the finite-rate chemistry proceeds. In the MILES_NS fine grid simulation, the turbulent time scale τ_t has been estimated to $\approx 5.10^{-6}$ s. The chemical time scale for air/H_2 stoichiometric chemistry is $\tau_c \approx 5.10^{-5}$ s. This gives a Damköhler number $\mathrm{Da} = \tau_t/\tau_c \approx 0.1$. Hence, there is a strong interaction between chemistry and turbulence in a thick flame region. The grid is mostly responsible for turbulent mixing. The finer the grid, the lower the subgrid-scale dissipation, either only numerical in MILES or numerical and explicit in LES. The residual numerical diffusion combines with molecular transport -except in MILES_EULER- to finally vary the mixture fraction across the diffusion layer and control the reaction rate.

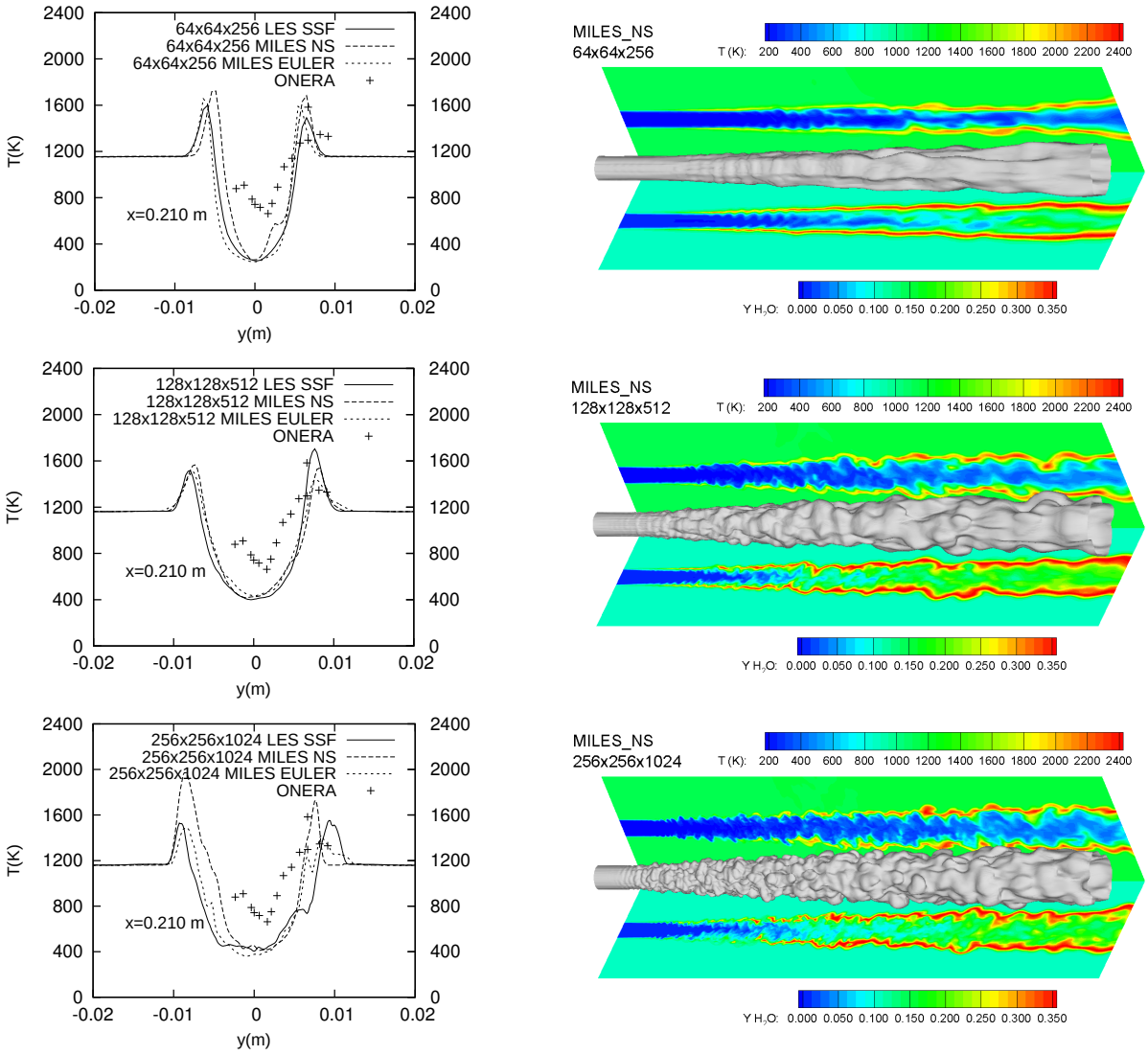

Figure 4. Left: averaged transverse temperature profiles at $x = 210$ mm. Right: instantaneous iso-surface z_{st}, temperature field and water mass fraction in the symmetry planes. Top to bottom: 64×64×256, 128×128×512, 256×256×1024.

Table 3. Relative cost of LES and MILES. Grid 128×128×512, 128 IBM Power6 CPU's. 0.2 ms of physical time simulated.

	Non-Reacting			Reacting		
	wall time	CPU/step	cost	wall time	CPU/step	cost
MILES_EULER	14238 s	508.4 s	**1**	73314 s	938.0 s	**1.845**
MILES_NS	16581 s	599.2 s	**1.178**	88540 s	1132.9 s	**2.228**
LES_SSF	16482 s	625.1 s	**1.229**	90284 s	1155.2 s	**2.272**
LES_SM	15680 s	603.6 s	**1.187**	—	—	—

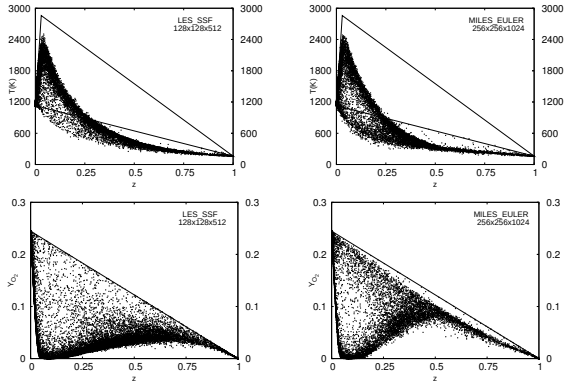

Figure 5. Scatter plots of temperature (top) and O_2 mass fraction (bottom). Left: LES_SSF 128×128×512, right: MILES_EULER 256×256×1024

The finite-rate detailed chemistry is clearly felt in figure 5 since the flame structure departs strongly from infinitely fast, irreversible one-step chemistry, equilibrium (straight) lines. The temperature mixing line is curved and below the theoretical linear mixing line because the hydrogen stream is very cold (160K, see table 2) and the heat capacity of hydrogen is very high (13200 J/kg.K at 160K) compared to that of air (1170 J/kg.K at 1200K). When hydrogen mixes with surrounding air, it takes heat from the oxidizer stream and lowers the mixture temperature below the self-ignition limit ($\approx$ 1000K at stoichiometry).

On the coarser grid (not shown), points are clustered close to the equilibrium states, indicating a higher Damköhler number. Few points can be found near the mixing line at $z \approx z_{st}$ because of a "mixed is burned" behavior: the strong numerical diffusion artificially brings reactants together at a pseudo-molecular level and reactions can complete. On the 128×128×512 grid, diagrams are more "filled", especially in LES_SSF (left column in figure 5), because turbulent mixing is faster and the reactive mixture can be found in various intermediate states combining reactants and products. More points can also be found near stoichiometry where reactions did not occur (high Y_{O_2}, low T) due to a "lack of time". Physical LES and MILES (not shown) give similar results. On the fine grid, the structure of the flame is slightly different. More points can be found close the mixing lines in the H_2 stream ($z \to 1$) where O_2 is present without reaction, because of the low temperature. Turbulent mixing is faster than chemistry, mainly in the MILES_EULER simulation (right column in figure 5) which differs clearly from LES_SSF: the low level of numerical diffusion and the absence of viscous model restrict the small scale molecular mixing, hence affect the reaction rates.

DISCUSSION AND CONCLUSION

The relative cost of the different simulations has been estimated for 0.2 ms of simulated physical time on the 128×128×512 grid, using 4×4×8 IBM Power6 processors. In the non-reacting case, the time step was limited by the CFL condition. In the reacting case the time step was limited to 2×10^{-8} s by chemistry. Table 3 indicates the total wall time for the simulation, the CPU time (single processor) per time step, and the normalized cost per time step. The reference is MILES_EULER non-reacting. In the non-reacting case, calculation of the molecular transport in MILES_NS represents an extra cost around 18%. The Smagorinsky model in LES_SM is hardly felt because velocity derivatives required in the model are already computed in viscous terms. The SSF model is a little more expensive due to the calculation of velocity differences and of the three-dimensionality sensor, but is also negligible. The 7 species, 14 reactions, chemistry in the reacting MILES_ EULER represent 85% of the WENO effort. Adding the transport model increases the cost up to 123%. The extra cost of the SSF model is negligible.

So, the choice of whether to introduce or not an explicit subgrid model in the simulation is not a matter of computational cost. MILES_NS performed with "clever" dissipative numerics provides almost the same grid-independent flow statistics as physical LES, for both non-reacting and reacting flows. In reacting MILES_EULER, a molecular viscous cutoff is mandatory to set a physical width for the reaction zone, in order to achieve grid convergence. In the non-reacting case however, grid convergence was observed, quite surprisingly. Further work should include a closure for subgrid chemical source terms.

This work was granted access to the HPC resources of IDRIS under the allocation 2010-020913 made by GENCI (Grand Equipement National de Calcul Intensif).

REFERENCES

Burcat, A. & Ruscic, B. 2006 Ideal gas thermodynamic data in polynomial form for combustion and air pollution use. Third Millennium Ideal Gas and Condensed Phase Thermochemical Database for Combustion [on line database].

David, E. 1993 Modélisation des écoulements compressibles et hypersoniques: une approche instationnaire. PhD thesis, Institut National Polytechnique de Grenoble, France.

Davidenko, D., Gökalp, I., Dufour, E. & Magre, Ph. 2006 Systematic numerical study of the supersonic combustion in an experimental combustion chamber. In *AIAA paper 2006-7913*, 14^{th} *AIAA/AHI International Space Planes and Hypersonic Systems and Technologies Conference*. Canberra, Australia, 6 - 9 November.

Eggers, J.M. 1971 Turbulent mixing of coaxial compressible hydrogen-air jets. *Tech. Rep.* NASA-TN-D-6487.

Erlebacher, G., Hussaini, M.Y., Speziale, C.G. & Zang, T.A. 1992 Toward the large eddy simulation of compressible turbulent flows. *Journal of Fluid Mechanics* **238**, 155–185.

George, E., Magre, Ph. & Sabel'nikov, V. 2006 Numerical simulations of self-ignition of hydrogen-hydrocarbons mixtures in a hot supersonic air flow. In *AIAA paper 2006-4611*, 42^{nd} *AIAA/ASME/SAE/ASEE Joint Propulsion Conference & Exhibit*. Sacramento, California, 9-12 July.

Grinstein, F.F., Margolin, L.G. & Rider, W.J. 2007 *Implicit Large Eddy Simulation : computing turbulent fluid dynamics*. Cambridge University Press.

Magre, Ph. & Sabel'nikov, V. 2002 Self-ignition of hydrogen-ethylene mixtures in a hot supersonic air flow. In *AIAA paper 2002-5205*, 11^{th} *AIAA/AAAF International Space Planes and Hypersonic Systems and Technologies Conference*. Orléans, France, 29 September - 4 October.